Cavitation erosion prediction by numerical cavitation

Cédric Flageul, Regiane Fortes Patella, Antoine Archer

CAVITATION EROSION PREDICTION BY NUMERICAL SIMULATIONS

Cédric Flageul[1], Regiane Fortes Patella[1]*, Antoine Archer[2]

[1] LEGI, Grenoble INP
BP 53 - 38041 Grenoble Cedex 9 – France
regiane.fortes@grenoble-inp.fr

[2] EDF - R&D Division
6, quai Watier BP49 – 78401 Chatou – France
Antoine.Archer@edf.fr

Abstract

A method is proposed to predict cavitation damage from cavitating flow simulations. For this purpose, a numerical process coupling cavitating flow simulations and erosion models was developed and applied to a two-dimensional (2D) hydrofoil tested at TUD (Darmstadt University of Technology, Germany) [1]. Two different erosion models were used and compared: the model proposed by Nohmi et al. [2] and the one developed in the LEGI laboratory [3,4].

Based on these models, two aggressiveness parameters were introduced and evaluated using CFD (Computational Fluid Dynamics) results. The simulated qualitative influence of flow velocity, sigma value and gas content on cavitation damage agreed well with experimental observations. Moreover, the downstream extent of cavitation erosion was correctly estimated, in particular by the LEGI model. On the other hand, significant discrepancies between simulated and experimental results were found for upstream unsteady cavitating flows. The CFD tool will have to be enhanced to improve simulation in this zone.

With the addition of some material parameters, the proposed methods were also able to predict volume damage rates corresponding to the incubation period of cavitation erosion.

Nomenclature

c_{min}: minimum speed of sound in the mixture = 1 m/s
$\boldsymbol{h_{agr}}$: height of integration for aggressiveness calculation (m)
L_{ref}: geometry reference length = 0.1 m
p: local static pressure (Pa)
p_{inlet}: inlet static pressure (Pa)
p_v: vapour pressure (Pa)
P_{g0}: pressure of non-condensable gas (Pa)
T_{ref}: reference time = L_{ref}/ V_{ref} (s)
V_{ref}: reference velocity= inlet velocity (m/s)
Vd: volume damage rate ($mm^3/m^2/s$)
α: void ratio $\alpha=\frac{(\rho-\rho_L)}{(\rho_V-\rho_L)}$ (-)
$\alpha*$: air content (ppm)
β: material coefficient (J/mm^3)
$\eta*$: collapse efficiency (-)
$\eta**$: hydrodynamic efficiency (-)
ρ: mixture density $\rho=\alpha\rho_V+(1-\alpha)\rho_L$ (kg/m^3)
ρ_l (=ρ_{ref}), ρ_v: liquid and vapour density (kg/m^3)
Cavitation number: $\sigma = \sigma_{inlet} = \frac{p_{inlet} - p_{vap}}{\frac{1}{2}\rho_{inlet}V_{inlet}^2}$ (-)
Aggressiveness parameters: (W/m^2)
LEGI model [3] : $P_{agr}^{LEGI} = \mathcal{P}_{pot}^{mat}/\Delta S$
Nohmi model [2] : P_{agr}^{Nohmi}

Introduction

Evaluation of the erosion power of cavitating flows and prediction of material damage remains a major concern for machinery manufacturers and users. Many studies have been carried out in recent years to improve knowledge on the cavitation erosion mechanism [1, 5-11]. For example, to predict the magnitude of cavitation damage, Kato et al. [7] proposed a scenario based on experimental results concerning cavitation generation rate, bubble distribution/collapse and impact force/pressure distribution.

From experimental work, Pereira et al. [9] found a relationship between the volume and rate of

* **Corresponding Author**

production of transient cavities and the material deformation energy.
Dular et al. [1] used data from the visualization of cavitation structures to predict the magnitude and distribution of cavitation damage. The proposed erosion model has since been coupled with a CFD code and tested on a 2D hydrofoil [12].
The approach developed by Steller and Krella [13] assumes that the material resistance to cavitation may be described satisfactorily by its response to individual fractions of the cavitation pulse amplitude distribution.
In most of those studies, experimental data are essential for the development and application of the proposed methods. However, experimental data are not always available, especially for complex geometries.
In this context, based on and improving on our previous work [3,4,8], the target of the present study is to propose and test models that are capable of predicting cavitation aggressiveness from cavitating flow simulations.
Two erosion models are considered: one proposed by Fortes-Patella et al. [3,4], described in section 1 and referred to as the LEGI model, and another proposed by Nohmi et al. [2], presented in section 2.
The idea is to calculate the cavitation aggressiveness parameter from unsteady cavitating flow simulations made using CFD codes. In this study, we consider a hydrofoil tested at TUD and described in section 3. Unsteady cavitating flow simulations have been carried out using an in-house two-dimensional code presented in section 4. The methodology applied to the analyses and the main results obtained are described in sections 5 to 8. The two erosion models are compared and the influence of certain numerical (time step) and physical parameters (air content, sigma value, flow velocity) are studied. Section 8 is devoted to the prediction of material damage, with the assessment of volume damage rates associated with cavitating flows.

1. The LEGI model

According to previous studies [4,8], pressure waves emitted during the collapses of vapour structures seem to be the main factor contributing to cavitation damage. The pressure waves can be generated either by spherical bubble or vortex collapses ([14] and [15]) or by micro jet formation [16]. The pressure waves interact with neighbouring solid surfaces, leading to material damage. Previous work [17] has indicated that material damage due to cavitation phenomena could be related to the characteristics (mainly the energy) of the pressure waves emitted by vapour structure collapses. In this context, the proposed model is based on the energy balance illustrated in Figure 1.

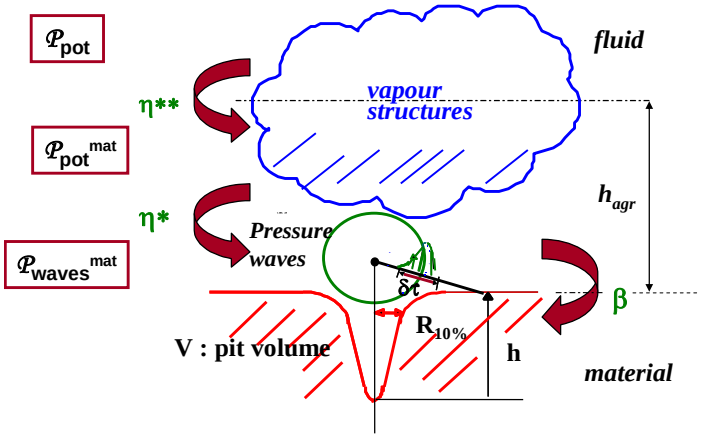

Fig.1 The physical scenario based on the energy balance: a pressure wave emitted during the collapse of vapour structures is considered to be the phenomenon responsible for material damage. The collapse of vapour cavities is characterized by the potential energy of the cavities (related to the pressure gradient and the cavity volume) and the collapse efficiency. The emitted pressure wave is characterized by its acoustic energy and the material damage is represented by the pit volume $V_{pit}=f(R_{10\%},H)$.

To evaluate the erosion power of a cavitating flow, we will introduce the notion of aggressiveness power densities.
Conventionally, the potential energy of a vapour structure is defined as the vapour volume V_{vap}, multiplied by a pressure imbalance:

$$\mathcal{E}_{pot} = \Delta P\, V_{vap} \qquad (1)$$

where $\Delta P=(P_\infty-P_{vap})$, P_∞ is the surrounding pressure and P_{vap} is the vapour pressure.
From this assumption, the instantaneous potential power can be defined by:

$$\mathcal{P}_{pot} = -\Delta P\, (dVvap/dt), \qquad (2)$$

We assume in equation 2 that the relative variation of the vapour volume is an order of magnitude higher than the ΔP variation and we can therefore neglect the term $\{Vvap\ (d(\Delta P)/dt)\}$. We assume that the vapour structure is aggressive if $\mathcal{P}_{pot}>0$. As

dVvap/dt <0, a minus sign is necessary in equation (2) to give positive potential energy values.
From unsteady results obtained by CFD, we evaluate the pressure, velocity, density fields and vapour volume in each cell of the calculated domain at every time step . These data can be used to evaluate $\mathcal{P}_{pot}$.
Inside a cell of volume V_{cell}, the vapour volume is related to the void fraction "α" by:

$$\alpha = V_{vap}/V_{cell}$$

and $\alpha = (\rho - \rho_l)/(\rho_v - \rho_l)$.
The potential energy density can be defined as:

$$\mathcal{P}_{pot}/V_{cell} = -\Delta P\,(d\alpha/dt) \qquad (3)$$

Note that we consider Lagrangian time derivatives in equations 2 and 3. From the local mass equation:

$$\partial\rho/\partial t + \mathrm{div}(\rho U) = 0 \quad \text{or} \quad d\rho/dt + \rho\,\mathrm{div}U = 0$$

We can thus deduce:

$$(\rho_v - \rho_l)\, d\alpha/dt = -\rho\,\mathrm{div}U$$

and

$$\mathcal{P}_{pot}/V_{cell} = -\Delta P\,\rho/(\rho_l - \rho_v)\,\mathbf{divU}$$

To evaluate cavitation aggressiveness, we take into account only the collapse phenomenon (i.e. when **divU<0)**.

The material is exposed to the collapses of neighbouring vapour structures. To characterize the aggressiveness intensity, an areal density can also be evaluated by integrating equation (3) to obtain:

$$P_{agr}^{LEGI} = \mathcal{P}_{pot}^{mat}/\Delta S = \int_{h\_agr} (\mathcal{P}_{pot}/V_{cell})\,dh \qquad (4)$$

where ΔS is the unit surface area and h_{agr} is the distance to the solid wall below which it is estimated that the structures are close enough to the wall to be aggressive. As a first approximation, based on Kato et al. [7], we consider h_{agr} equal to 10% of the thickness of the attached cavitation sheet.
The influence of the distance of vapour structures from the wall could also be taken into account by a dimensionless function, f(h/h_{agr}), under the integral sign. This will be developed in a subsequent paper.
The distance h_{agr} is in fact related to the efficiency η** introduced in the energy balance illustrated in Figure 1:

$$\mathcal{P}_{pot}^{mat}/\Delta S = \eta^{**}\,\mathcal{P}_{pot}/\Delta S$$

This efficiency is a function of the hydrodynamic characteristics (V_{ref}, σ) of the flow and depends on the distance between the vapour structure collapse and the solid surface. It is mainly influenced by the type, unsteadiness and geometry of the cavitating flow, depending for example on the angle of attack and the shape of the leading edge for a hydrofoil.

2. The Nohmi model [2]

Based on the qualitative information obtained from the Rayleigh-Plesset equation coupled with flow field CFD, Nohmi et al., [2] have proposed different parameters to characterize cavitation aggressiveness. The proposed parameters depend on the void ratio (i.e. the number of bubbles) and the pressure over the solid surface. They can be evaluated directly from homogeneous cavitating flow field calculations using the relation:

$$P_{agr}^{Nohmi} = \left(-\frac{\partial^{N1}\alpha}{\partial t^{N1}}\right)^{N2}\left(\frac{\partial^{N3}(p-p_v)}{\partial t^{N3}}\right)^{N4} \qquad (5)$$

with $\alpha>0$, $\partial_t\alpha<0$ and $p>p_v$.
To apply this model, we need to choose values for the parameters N1 to N4. In the present paper, we use the following aggressiveness parameter:

$$P_{agr}^{Nohmi} = \max\left(0,-\frac{\partial\,\alpha}{\partial t}\right)\max(0,p-p_v) + \alpha\max\left(0,\frac{\partial\,(p-p_v)}{\partial t}\right) \qquad (6)$$

Other representations of aggressiveness can be defined using the parameters N1 to N4.
Note that equations (3) and (6) have the same dimensions [W/m^3], allowing an easier comparison with the LEGI model.
Based on the CFD calculations presented in section 4, both approaches have been implemented, analyzed and compared. Qualitative comparisons with available experimental data have also been carried out.

3. Hydrofoil geometry

The geometry considered in this study is a 2D hydrofoil with a semicircular nose (Fig. 2 and 3). This geometry has been tested at Darmstadt University of Technology [1,18,19]. Different visualisation techniques and velocity (PIV) and pressure measurements have been used. Several configurations of cavitating flow have been tested (upstream cavitation numbers varying between 2 and 3.5, flow velocities of 13 m/s and 16 m/s and air contents from 14.3 ± 0.5 mgg/lw (milligrams of gas per litre of water) to 48.5 ± 0.7 mgg/lw). Pitting tests

on copper samples have been also carried out for this geometry by Lohrberg et al. [20].
Experimental work indicates an influence of the lateral walls and results show 3D cavitation structures. Nevertheless, despite the recent progress in the area of computational fluid dynamics, 3D unsteady calculation of cavitating flow is very time consuming. Therefore, we follow a 2D approach in this paper.

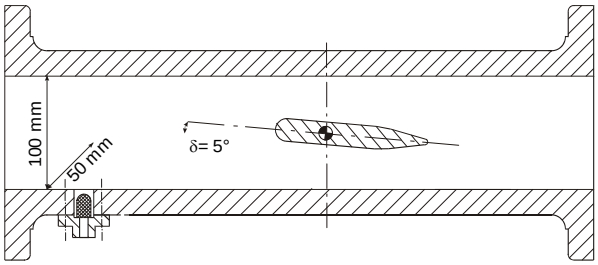

Fig.2 Test-section in a closed loop [18].

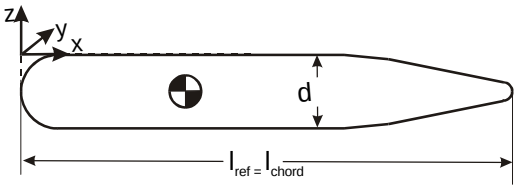

Fig.3 Hydrofoil [18] (l_{chord}=0.1079m; d=16 mm).

4. CFD code

To simulate the unsteady cavitating flow in this geometry, we have applied the in-house 2D code referred to as "IZ", developed with the support of the CNES-Centre National d'Etudes Spatiales.
Reynolds Averaged Navier-Stokes equations are solved for a homogeneous fluid with variable density:

$$\frac{\partial \rho_m}{\partial t} + \nabla\left(\rho_m \mathbf{u}_m\right) = 0$$

$$\frac{\partial \rho_m \mathbf{u}_m}{\partial t} + \nabla\left(\rho_m \mathbf{u}_m \otimes \mathbf{u}_m\right) = -\nabla(p_m) + \nabla(\bar{\bar{\tau}}_m)$$

where $\bar{\bar{\tau}}_m$ is the shear stress tensor and ρ_m is the mixture density, defined with respect to the void ratio α as:

$$\rho_m = \alpha\ \rho_v + (1-\alpha)\rho_L$$

The applications concerned are for cold water. Calculations do not take into account thermodynamic effects and the energy equation is not solved. Two phases are considered to be locally (in each cell) in dynamic equilibrium (no drift velocity). Each pure phase is considered incompressible.
A finite volume spatial discretization is applied in curvilinear orthogonal coordinates on a staggered mesh. An iterative resolution based on the SIMPLE algorithm was developed to deal with quasi-incompressible flow (α=0 and α=1) and highly compressible flow (0< α<1). The liquid–vapour interfaces are described by high gradients of the mixture density ρ_m (hereafter simply denoted ρ), made possible by the use of a conservative approach and the HLPA non-oscillatory second order MUSCL scheme [21].
To solve the time-dependent problem, first or second order fully implicit methods are available. In most of the calculations, the time step "dt" is equal to 0.0032 T_{ref} and the calculation duration about 80 T_{ref} (which makes it possible to simulate more than 150 cloud shedding cycles). The influence of "dt" is analysed in section 8.
Turbulent flows are calculated by solving the Reynolds equations using a modified k-ε RNG turbulence model with standard wall functions. The modified k-ε RNG turbulence model has been described in detail by Coutier-Delgosha et al. [22].
To model the cavitation phenomenon and to close the governing equations system, a barotropic state law was used [23]. The fluid density (and thus the void fraction) is controlled by a $\rho(p)$ law that explicitly links the mixture fluid density to the local static pressure. This law is mainly controlled by its maximum slope, which is related to the minimum speed of sound c_{min} in the mixture. In the present study, c_{min} = 1 m/s. The CFD code has already been validated on numerous experiments and has been widely described [22,24].
Figure 4 illustrates the computational H-grid applied in the present study. It is composed of (250 x 80) orthogonal cells. At the first grid points, to use standard laws for the walls, the dimensionless parameter y+ of the boundary layer varies between ~20 and 50 under non-cavitating conditions.
Concerning other boundary conditions, the code takes into account circuit impedance and permits the use of non-reflecting boundary conditions [25]. More usual incompressible boundary conditions (imposed inlet flow velocity and outlet pressure) are also available. Influence tests concerning barotropic law

parameters and meshing will be dealt with in subsequent work.

5. Methodology of analysis

The CFD simulation provides the void ratio, pressure and divergence of the velocity. The values on the top of the hydrofoil are extracted for each time step. They will be used to calculate the cavitation aggressiveness. The first step in the analysis is to determine the length of the initial transient flow. The total volume of vapour in the flow is a good indication. Figure 5 shows an initial transient flow lasting ~20 T_{ref} and a periodic flow lasting ~60 T_{ref}. LEGI aggressiveness is calculated at each time step during the periodic part. Nohmi aggressiveness involves a time derivative and is calculated at $(t^i+t^{i+1})/2$ using CFD values at t^i and t^{i+1} (first order scheme).

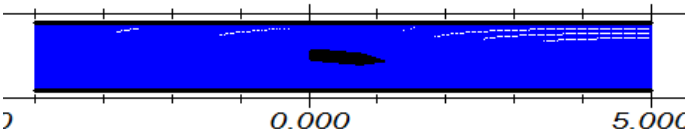

Computational domain

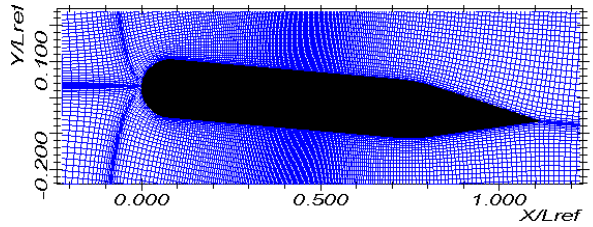

Zoom of the mesh close to the hydrofoil

Fig. 4 H-grid (250 x 80) orthogonal cells.

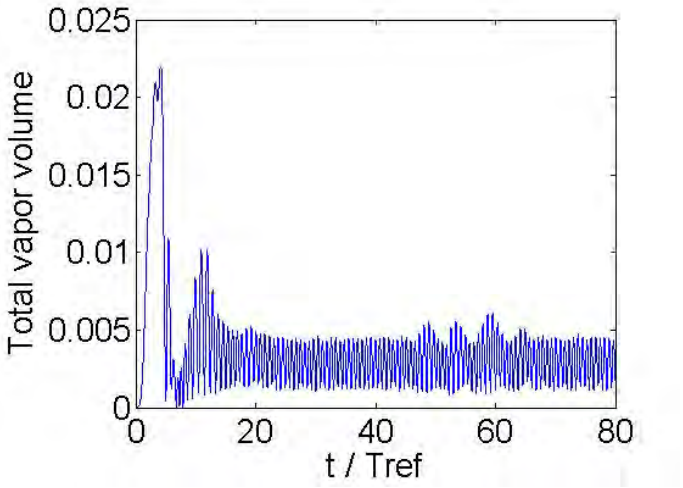

Fig.5 Evolution of the simulated total vapour volume ($/L_{ref}^3$) in the flow (V_{ref}=13m/s, $\sigma_{upstream}$=2.3).

Knowing $\mathcal{P}_{pot}$, h_{agr} is needed to calculate $\mathcal{P}_{pot}^{mat}$. Flow visualization can be used to estimate the attached cavity length L_{cav} and thickness h_{cav}. Based on Kato et al. [7], we used h_{agr} =(10% h_{cav}). Using this value, both LEGI and Nohmi aggressiveness can be integrated over the hydrofoil (equation 4). Finally, the instantaneous aggressiveness can be integrated using the simulation's time step. Mean aggressiveness is obtained by dividing the result by the length of the periodic part of the flow.

For this example, V_{ref}=13m/s, σ=2.3 and h_{agr}=(10%h_{cav})=108 μm. Results concerning mean aggressiveness parameters are presented in Fig. 6 and 7.

Note that numerical simulations lead to a good prediction of the cloud shedding process, frequency and mean velocity profiles. Conversely, CFD unsteady results near the leading edge ($x<0.2L_{ref}$) disagree with experimental visualizations and the damage predicted in this area is overestimated. CFD tools must be improved to obtain a better simulation in this zone. In the present paper, we present the analyses concerning the real damage zone observed experimentally on the hydrofoil surface (i.e. $x\geq0.2L_{ref}$).

6. Influence of the distance h_{agr}

The distance h_{agr} is an important parameter. Vapour structures close to the wall are more likely to be erosive than those further away. Figure 6-7 shows that aggressiveness increases with h_{agr}. Vapour structures imploding far away from the wall affect the shape of the aggressiveness for h_{agr} values of ~1.7 mm and 2 mm. Such structures may not be very erosive, leading to an overestimation of the aggressiveness. Moreover, for high values of h_{agr}, no distinction can be made between the area where real damage does and does not occur ($x<0.2L_{ref}$).

Figures 6 and 7 indicate some differences between the aggressiveness models. These differences appear for every h_{agr}, even if only the first cell is taken in account in the post-processing (h_{agr}=0.0108mm).

For a given value of h_{agr}, the maximum aggressiveness amplitude is higher for the Nohmi model (but the order of magnitude of the amplitudes is similar for both models).

Comparison of the aggressiveness shape and extension obtained by numerical simulations and

experiments carried out by Dular and Coutier-Delgosha [12] indicates a better prediction by the LEGI model with $h_{agr} \leq 0.108$mm.
Complementary experimental and numerical studies are currently being pursued in EDF and LEGI laboratories to improve the analysis of h_{agr} influence.

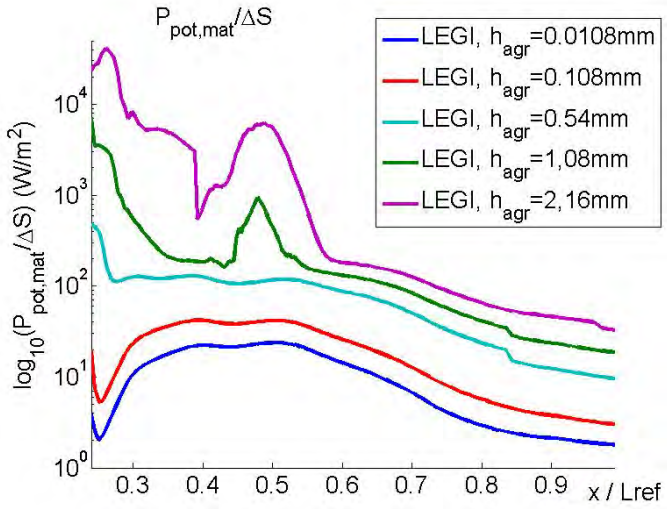

Fig.6 Influence of h_{agr} on LEGI cavitation aggressiveness calculated on the hydrofoil surface (V_{ref}=13m/s, σ=2.3).

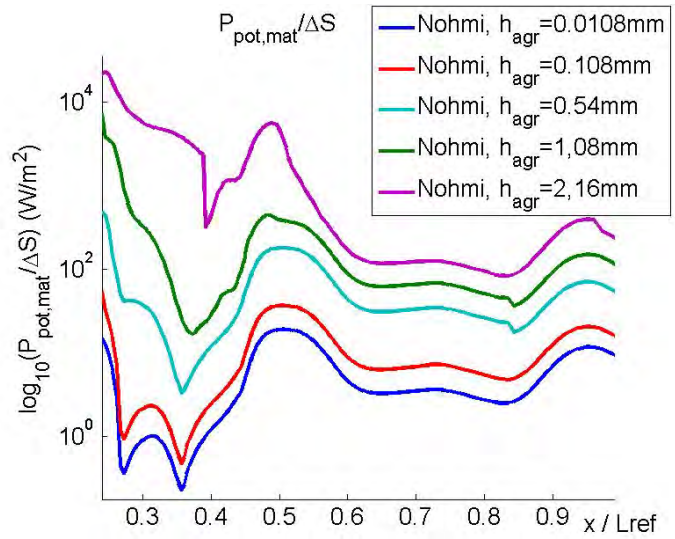

Fig.7 Influence of h_{agr} on Nohmi cavitation aggressiveness (V_{ref}=13m/s, σ=2.3).

7. Influence of the time step

Figures 8 and 9 show the influence of the time step on the prediction of cavitation aggressiveness for the two models. For the LEGI model, the mean aggressiveness increases with the time step, but the damage extension is not affected.

On the other hand, for the Nohmi model, the shape and amplitude of aggressiveness are highly dependent on the time step. The Nohmi model may be more sensitive to the time step because aggressiveness calculations involve time differentiation. The simple first order scheme may be partly responsible for this. LEGI cavitation aggressiveness therefore appears to be more robust regarding the influence of the time step.

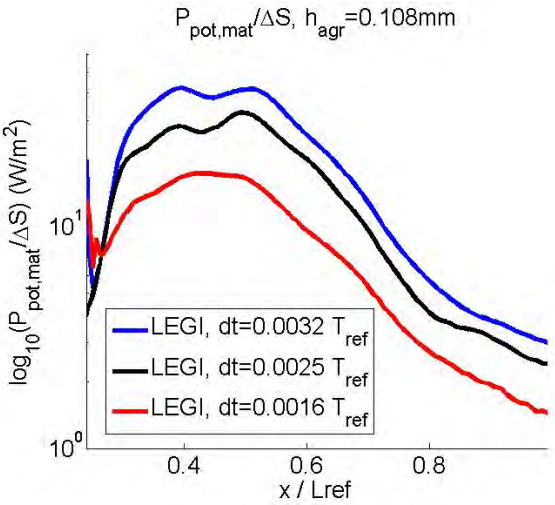

Fig.8 Influence of the time step on LEGI cavitation aggressiveness (V_{ref}=13m/s, σ=2.3).

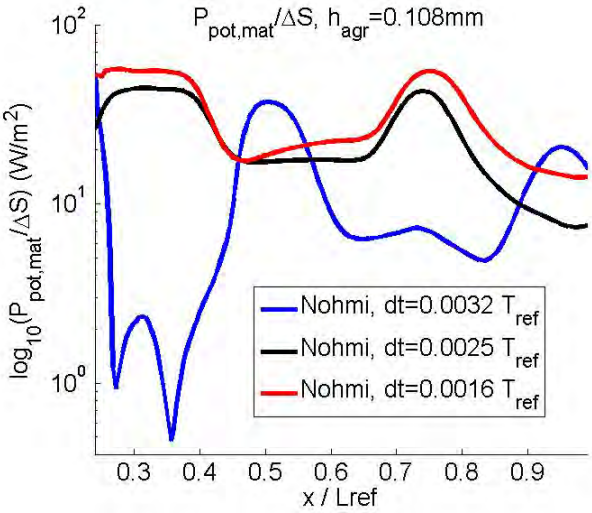

Fig.9 Influence of the time step on Nohmi cavitation aggressiveness (V_{ref}=13m/s, σ=2.3).

8. Damage prediction

Based on the scenario proposed in Figure 1, the global model allows prediction of material damage

from cavitating flow simulations. We assume that pressure waves emitted during vapour structure collapses are the phenomenon responsible for damage. The energy of erosive vapour structures existing in the flow are associated with the aggressiveness parameter $\mathcal{P}_{pot}^{mat}/\Delta S$ calculated above (by the LEGI or Nohmi model).

When these structures collapse, pressure waves are emitted, with a power density applied to the material given by:

$$\mathcal{P}_{waves}^{mat}/\Delta S = \eta^* \mathcal{P}_{pot}^{mat}/\Delta S \qquad (7)$$

where the efficiency η* is modelled by the collapses of spherical bubbles of vapour and gas. In a previous study [26], the efficiency of the collapse η* (defined as the ratio between pressure wave energy and initial bubble energy) was evaluated for different bubble implosions by means of Keller's as well as Fujikawa and Akamatsu's physical models [27,28]. According to these authors, η* depends mainly on the local liquid pressure P_∞ and on the initial gas pressure P_{go} within the bubble, as indicated in Figure 10. Note that the initial gas pressure P_{g0} is related to the air content in the liquid. Brennen [29] has proposed a theoretical model for gas convection from a cavity interface which gave the following linear relation between P_{g0} and $\alpha*$:

$$P_{g0} \sim 69\ \alpha* \text{ (Pa)}$$

where $\alpha*$ is the air content (ppm), considered to be known and constant for a given cavitating flow.

Hence, based on the areal power density $\mathcal{P}_{pot}^{mat}/\Delta S$, the local P_∞ calculated from CFD and on the efficiency η* evaluated from Figure 10 (for a given P_{g0} value), we can evaluate the power density $\mathcal{P}_{waves}^{mat}/\Delta S$ from equation 7.

During the incubation period of the cavitation erosion phenomenon (i.e. without mass loss), the impact of a pressure wave leads to plastic deformation of the material characterized by a deformed volume V_{pit}. Following the proposed physical scenario (Fig. 1) and taking into account energy transfers between the pressure wave and material damage [4], we assume that:

$$\mathcal{P}_{waves}^{mat}/\Delta S = \beta\, Vd$$

and

$$\mathcal{P}_{pot}^{mat}/\Delta S = \beta\, Vd/\eta^*$$

where Vd is the volume damage rate (i.e. the deformed volume divided by the analyzed sample surface area and test duration) and β is a mechanical characteristic of the material evaluated by numerical simulations (for copper, $\beta_{copper} \sim 20\ (\pm 2)$ J/mm^3). For more details, see [4].

Figures 11 to 13 present damage prediction for some of the analyzed cases using the LEGI model. Different air contents, cavitation numbers and flow velocities have been considered.

Fig. 14 and 15 illustrate some qualitative comparisons between numerical and experimental results obtained by Dular and Coutier-Delgosha [12]. Qualitative results are in very good agreement with experimental results concerning the influence of air content and flow velocity [1]. A classical power law relating cavitation aggressiveness to the flow velocity is obtained (maximum value of $Vd \sim v^{4.3}$).

Concerning air content (Fig. 12), the proposed model leads to an attenuation of aggressiveness with increasing air content. The presence of non-condensable gas inside the fluid reduces the amplitude of pressure waves emitted during vapour structure collapses.

The qualitative influence of the sigma number also seems to be well simulated (Fig. 13), but the erosion area predicted by σ=2 does not agree well with the experimental value [12] (mainly in the upstream zone) and we have to improve the calculations and the analyses for this case.

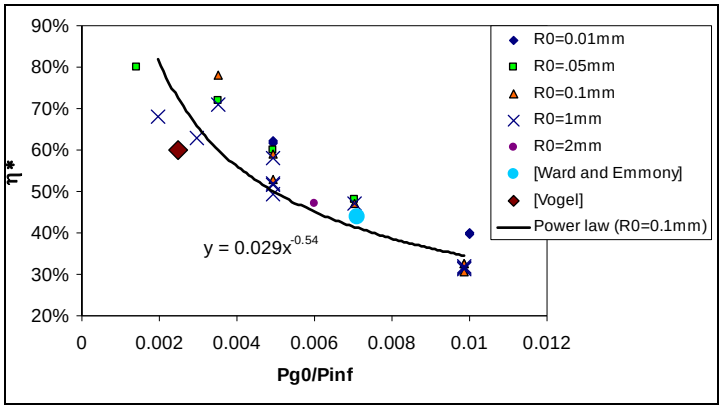

Fig.10 Collapse efficiency as a function of P_{g0}/P_∞ for different initial bubble radii. Results from [14] and [15] are also plotted.

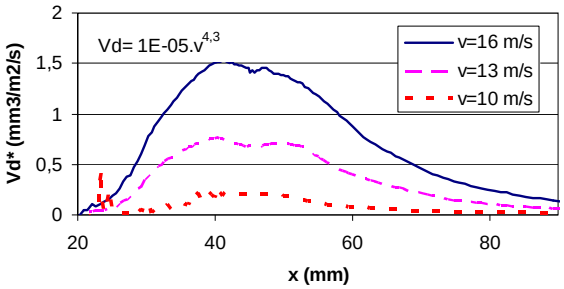

Fig.11 Influence of the flow velocity. For these calculations, σ=2.3; h_{agr} =150 µm; P_{g0}=500 Pa (35%<η*<58%).

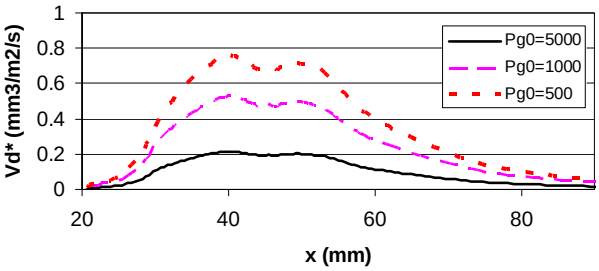

Fig.12 Influence of air content. For these calculations, V=13 m/s; σ=2.3; h_{agr}=150 µm; 13%<η*<46%.

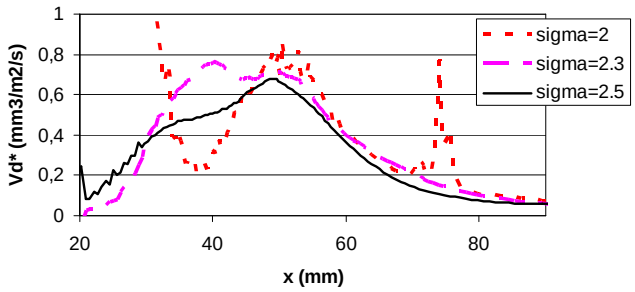

Fig.13 Influence of sigma values. For these calculations, V=13 m/s; h_{agr}=200 µm (σ=2); h_{agr}=150 µm (σ=2.3); h_{agr}=120 µm (σ=2.5); P_{g0}=500 Pa (η*~46%)

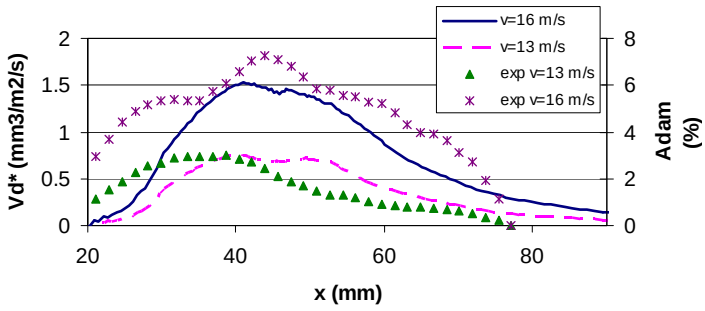

Fig.14 Flow velocity effect. Qualitative comparisons between experimental [12] and numerical results. A_{dam} is given by the ratio between pit areas measured after 1 hour of exposure to cavitating flow and a reference area.

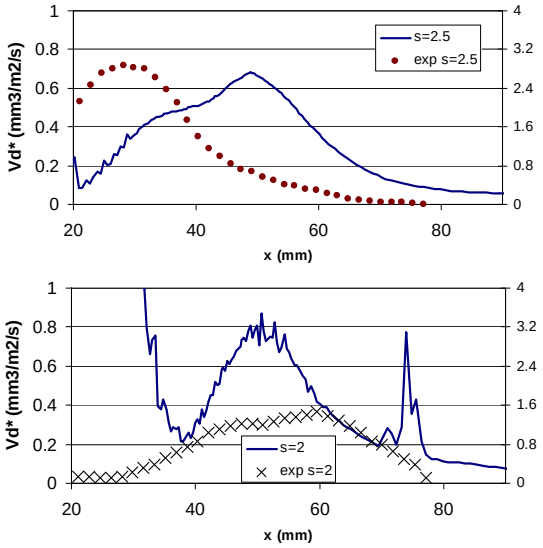

Fig.15 Sigma values influence. Qualitative comparisons between experimental [12] and numerical results.

Conclusion

A physical scenario allowing the prediction of cavitation damage from CFD simulations has been proposed. For this initial application, two erosion models were implemented and tested on a 2D hydrofoil geometry. Note that the proposed methodology can be associated with others CFD tools allowing reliable unsteady simulations of cavitating flows in 2D or 3D geometries.

The influence of physical parameters such as sigma value, flow velocity and air content has been evaluated and explained. A very good qualitative agreement between simulations and experiments was found for the geometry considered. To obtain a better quantitative prediction of damage, some numerical and model parameters have to be calibrated and tested for other geometries and cavitating flow conditions. For this, further experimental work including trustworthy pitting tests and air content control are needed and will be carried out in the near future in our laboratories.

In any case, the proposed erosion models, associated with CFD tools, represent a promising approach to predict and control cavitation erosion damage in real hydraulic systems and machinery.

Acknowledgements

This study was supported by the R&D Division of EDF (Electricité de France). Concerning the numerical aspects of this work, the authors would like to express their

gratitude to the CNES (French Space Agency) for their continuous support.

References

[1] Dular M., Stofel B., Sirok B., 2006, “Development of a cavitation erosion model”, *Wear*, 261, 642-655.
[2] Nohmi M., Ikohagi T., Iga Y., 2008, “Numerical prediction method of cavitation erosion”, *Proceedings of FEDSM2008*, Jacksonville, USA.
[3] Fortes-Patella R., Reboud JL., Briançon-Marjollet L., 2004, “A Phenomenological and numerical model for scaling the flow aggressiveness in cavitation erosion”, *Cavitation Erosion Workshop*, Val de Reuil, May 2004.
[4] Fortes Patella R., Challier G., Reboud JL., Archer A., 2001, "Cavitation erosion mechanism: numerical simulations of the interaction between pressure waves and solid boundaries", *Proceedings of CAV 2001 Symposium*, June 2001, Pasadena.
[5] Franc J.P., Michel J.M., Nguyen-Trong H., Karimi A., 1994, "From Pressure Pulses Measurements to Mass Loss Prediction: The Analysis of a Method", *Proc. 2nd Int. Symp. on Cavitation*, Tokyo, pp. 231-236.
[6] Lecoffre Y., 1995, "Cavitation Erosion, Hydrodynamics Scaling Laws, Practical Method of Long Term Damage Prediction", *Proceedings of. Int. Symp. on Cavitation, CAV’95*, Deauville, pp. 249-256.
[7] Kato H., Konno A., Maeda M., Yamaguchi H., 1996, "Possibility of Quantitative Prediction of Cavitation Erosion Without Model Test", *Journal of Fluid Engineering , Transactions of the ASME*, Vol. 118, pp. 582-588.
[8] Fortes-Patella R., Reboud JL., 1998, "A New Approach to Evaluate the Cavitation Erosion Power", *Journal of Fluid Engineering , Transactions of the ASME*, Vol. 120, June 1998.
[9] Pereira F., Avellan F., Dupont J.M., 1998, "Prediction of Cavitation Erosion: an Energy Approach", *Journal of Fluid Engineering , Transactions of the ASME*, Vol. 120, December 1998.
[10] Hattori S., Hirose T., Sugiyama K., 2010, “Prediction method for cavitation erosion based on measurement of bubble collapse impact loads”, *Wear* 269, 507–514.
[11] Franc J. P., 2009, “Incubation time and cavitation erosion rate of work-hardening materials”, *Journal of Fluids Engineering*, *131*, 021303.
[12] Dular M., Coutier-Delgosha O., 2009, “Numerical modelling of cavitation erosion”, *Int. J. Numer. Meth. Fluids*, 61:1388–1410.
[13] Steller J., Krella A., 2007, “On fractional approach to assessment of material resistance to cavitation”, *Wear* 263, 402–411.
[14] Vogel A., Lauterborn W., Timm R., 1989, "Optical and Acoustic Investigations of the Dynamics of Laser-Produced Cavitation Bubbles Near a Solid Boundary ", Journal of Fluid Mechanics, Vol. 206, pp. 299-338.
[15] Ward, Emmony, 1990, "The Energies and Pressures of Acoustics Transients associated with Optical Cavitation in Water", *Journal of Modern Optics*, vol.37, number 4.
[16] Philipp A., Ohl C. D., Lauterborn W., 1995, "Single Bubble Erosion on a Solid Surface", *Proceedings of Int. Symp. on Cavitation-CAV’9*5, Deauville, pp. 297-303.
[17] Fortes-Patella R., Reboud JL,1998, "Energetical Approach and Impact Efficiency in Cavitation Erosion", *Proc. of 3rd International Symp. on Cavitation*, Grenoble.
[18] Hofmann M., Lohrberg H., Ludwig G., Stoffel B., Reboud J.L, Fortes-Patella R., 1999, “Numerical and experimental investigations on the self-oscillating behaviour of cloud cavitation: Part I: Visualisations“, *FEDSM99-6755, 3rd ASME/JSME joint Fluid Eng. Conf*., July 1999, San Francisco.
[19] Reboud JL., Fortes-Patella R., Hofmann M., Lohrberg H., Ludwig G., Stoffel B., "Numerical and experimental investigations on the self-oscillating behaviour of cloud cavitation: Part two: Dynamic pressures", *FEDSM99-7259, ASME/JSME joint Fluid Eng. Conf*., July 1999, San Francisco.
[20] Lohrberg H., Hofmann M., Ludwig G., Stoffel B., 1999, "Analysis of Damaged Surfaces: Part II: Pit Counting by 2D Optical Techniques", *Proc. of the 3rd ASME/JSME Joints Fluids Engineering Conference*, July, San Francisco.
[21] Zhu J., 1991, "A low diffusive and oscillation-free convection scheme", *Comm. in Applied Num. Methods*, vol. 7.
[22] Coutier-Delgosha O., Fortes-Patella R., Reboud J.L., 2003, "Evaluation of the turbulence model influence on the numerical simulations of unsteady cavitation", *J of Fluids Eng*., Vol. 125 pp. 38-45.
[23] Delannoy Y., Kueny J.L., 1990, “Two phase flow approach in unsteady cavitation modelling”, *Cavitation and Multiphase Flow Forum*, ASME-FED vol 98, pp 153-158.
[24] Coutier-Delgosha O., Reboud J-L., Delannoy Y., 2003, "Numerical simulation of the unsteady behaviour of cavitating flows", *Int. J. for Numerical Meth. In fluids*, Vol. 42, pp. 527-548.
[25] Pouffary B., Reboud JL., Fortes-Patella R., 2004, "Unsteady cavitating flows in turbomachinery: comparison of two numerical models and applications", *Proceedings of ECCOMAS2004 Symposium*, invited lecture, July 2004, Finland.
[26] Fortes-Patella R., Challier G., Reboud JL., 1999, "Study of Pressure Wave Emitted During Spherical Bubble Collapse", *Proc. of the 3rd ASME/JSME Fluids Eng. Conference*, July, 1999, San Francisco, California.
[27] Fujikawa S., Akamatsu T., 1980, "Effects of Non-Equilibrium Condensation of Vapor on the Pressure Wave Produced by Collapse of a Bubble in Liquid", *Journal of Fluid Mechanics*, Vol. 97-3, pp.481-512.
[28] Prosperetti, Lezzi, 1986, “Bubble Dynamics in a Compressible Liquid. Part I: First Order Theory”, *Journal of Fluid Mechanics*, vol 168, pp 457-478.
[29] Brennen, 1969, "The Dynamic Balances of Dissolved Air and Heat in Natural Cavity Flows", *Journal of Fluid Mechanics*, vol 37, part 1, pp 115-127.